GeoConvention
Calgary • Canada • March 7-11 2016
OPTIMIZING RESOURCES

Microseismic Calibration of a Geomechanical Simulation of a Horn River Basic Hydraulic Fracture Treatment

Shawn Maxwell, Byungtark Lee and Mark Mack
IMaGE

Summary

A coupled hydraulic-geomechanical simulation is used to model hydraulic fracture growth and predict the corresponding microseismicity. Using a case study from the Horn River Basin, a quantitative match between the modeled and observed microseismic deformation is used to calibrate a reconstruction of the hydraulic fracture network that reconciles the geological and geomechanical earth model with the fracture engineering. The calibrated fracture model includes an estimate of the propped portion of the fracture network and can then be used to investigate alternate designs to optimize the well, completion and injection to maximize the conductive fracture and thereby reservoir drainage.

Introduction

Exploitation of unconventional reservoirs requires an effective hydraulic fracture stimulation to enhance flow in low permeability formations. Hydraulic fracture growth typically involves creation of new tensile fractures and interactions with pre-existing planes of weakenss in the reservoir, resulting in complex fracture networks. The hydraulic fracture growth is driven by the interplay between pressure diffusion and mechanical deformation, ultimately controlled by the dynamic hydraulic and geomechanical characteristics of the reservoir. The hydraulic and geomechanical factors are closely coupled, such that the high pressure fluids can cause fractures to dilate thereby enhancing flow and changing the pressure distribution. Localized fracture deformation can occur directly on the pressurized fractures as well as at more remote locations with the associated stress field perturbations.

The geomechanical component of the fracture growth can lead to inelastic strain and associated microseismicity that is commonly monitored to image the hydraulic fracture network. The microseismicity represents one specific component of the geomechanical deformation, often the instantaneous shear fracture slip along pre-existing planes of weakness. Nevertheless, the microseismicity provides important geomechanical information about the dynamic geomechanical processes. Understanding the coupled geomechanical and hydaulic processes is key to understanding the fracture geoemetry and contact with the reservoir and more crucially the proppant placement and associated enhanced permeability. Ultimately, a customized hydraulic fracture design can be defined for specific reservoir conditions to both enhance production and optimized operational costs.

Method

A coupled hydaulic-geomechanical model (3DEC, Damjanac and Cundall, 2014) is used to examine hydraulic fracture growth (Maxwell et al., 2015) through a discrete fracture network (DFN). A mechanical model is constructed, with zoned elastic properties and an initial stress state. The DFN is specified and the software constructs an adaptive grid assoicated with each fracture segment and the enclosed blocks. Mechanical properties of frictional strength and cohesion is defined for each fracture. The model honors the fluid injection rate and volume and simulates the flow of the fracturing fluid within the reservoir, including the proppant. The injected fluid and associated net pressure results in dynamic mechanical deformation, which can be either through creation or extension of new fractures or activation of pre-existing fractures. At each time step, flow is computed based on the pressure distribution and the corresponding fracture state

computed based on unbalanced forces. The mechanical state is examined including associated stress changes from the hydraulically driven fracture deformation, along with the stability of each fracture segment. Depending on the updated stress conditions, a mohr-colomb failure criteria is assessed such that fractures can deform in either a mode 1, mode 2 or combination of the two depending on the unbalanced forces. Once 'sealed' fractures slip, they become potential future flow channels. Associated with fracture slip, seismic source characteristics are assessed across multiple time steps and flagged as a microseismic event provided that slip is sufficiently rapid and there is sufficient confinement to create detectable seismic energy. Seismic moment of the slip are computed and the mechanism of slip defined and stored for these synthetic microseismic events.

In this way, the 3DEC model is able to replicate a geologic model of the reservoir and simulate hydraulic fracture growth. The simulation can be compared with observed net pressure as well as by matching the synthetic microseismicity with that detected in the field. The model can then be calibrated to the field observations by adjusting uncertain model parameters, particularly the DFN, to improve the match with field diagnostics. The calibrated model can then be investigated to optimize the engineering design to maximize reservoir contact for optimal production and minimal operational costs.

Example

A case study from the Horn River Basin (Rodinov et al., 2012) is presented to highlight the model calibration. Stage 5 of the project was investigated to construct a calibrated hydraulic fracture model. Figure 1 shows the stress variations with depth, computed by integrating the density log to calculate the vertical stress. The associated mininum stress estimated from Poisson's ratio determined from a dipole sonic log and calibrated with the ISIP. The maximum stress was computed to create an assumed strike-slip stress regime.

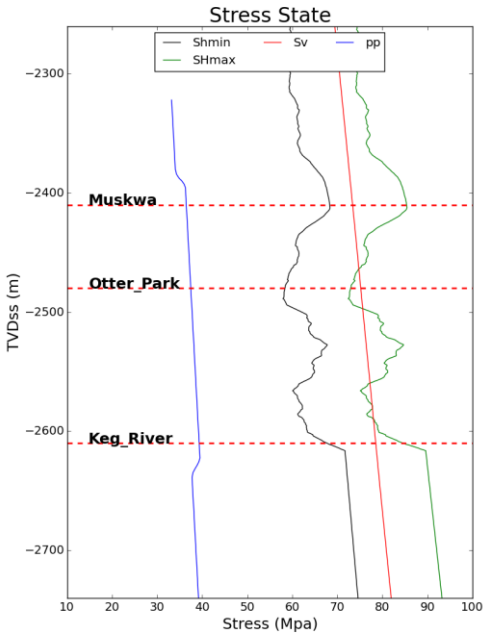

Figure 1. Stress profile.

A DFN was constructed based on a microseismic source mechanism analysis using reported amplitude ratios. Source mechanisms identified fractures subparallel to SHmax direction. Fracture dimensions and density were also estimated from the microseismicity. A DFN representation was constructed using these fracture characteristics. A combination of total organic content and clay can be used to define the fracture friction angle (e.g. Kohli and Zoback, 2013)and all fractures were initially assumed to be hydraulically sealed with a constant cohension.

The stage had three perforation clusters separated by 25 m, and a 95 minute injection at a rate of 9.6 m^3/min was simulated. A low leakoff coefficient was used to represent fluid loss to the matrix.

The first step of the calibration is to determine the fracture height with a consistent seismic moment depth distribution, by running the simulation using these starting parameters. Figure 2 shows the resulting aperture of the primary fractures from each cluster and the corresponding comparison of seismic moment between the model and field observations. The model is expected to produce slightly higher moment, since the field events is never expected to record all the deformation. A good match is found for both the depth and lateral distribution of moment.

Figure 3 shows a map view of the observed and modeled microseismicity. Not only the extent of the microseismicity but also the general character of the microseismicity is representative suggesting realism of the model. In the microseismic comparison, modeled locations have been statistically perturbed based on the reported location accuracy of the field data. This has the effect of spreading the events out consistent with the resolution of the real microseismic image.

Figure 4 shows the distubtion of fracturing fluid in different parts of the model, mostly in the primary hydraulic fracture and only 4% in the DFN. This is in contrast to other modeling examples where a relatively higher proportion of the fluid is found in the DFN. Not only is the fluid content low in the pre-existing fractures but there is also not sufficient aperture to allow proppant to enter the fractures. The model shows the proppant is soley contained in the primary hydraulic fractures. Figure 5 shows the primary fractures for each perforation cluster and the corresponding proppant thickness (i.e. concentration). There are regions of increased proppant concentration mainly in the Muskwa interval but some in the upper Otter Park.

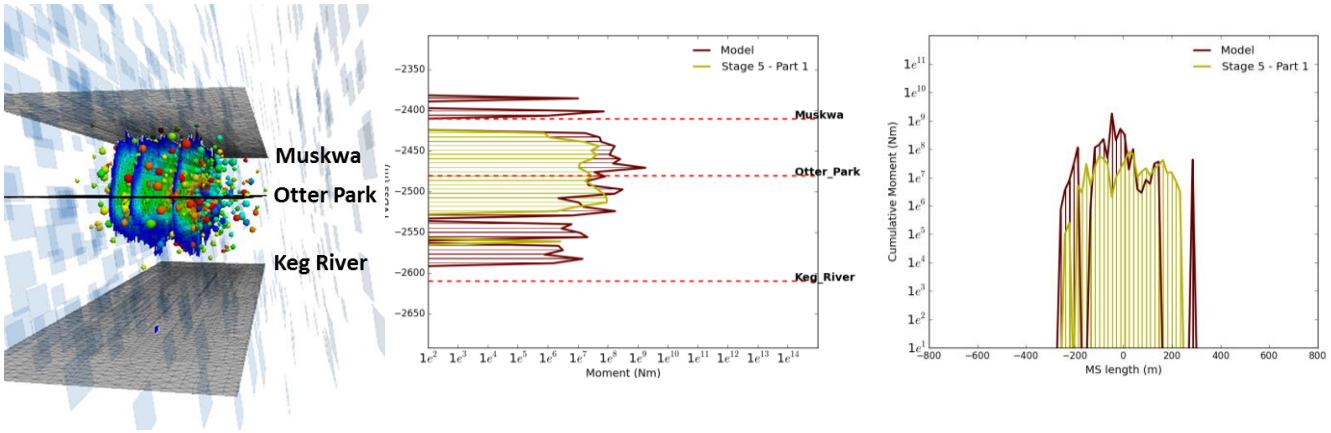

Figure 2. Perspective view of primary fractures and synthetic microseismic (left). Depth (center) and lateral (right) distribution of moment release from the model (red) and observed (green)

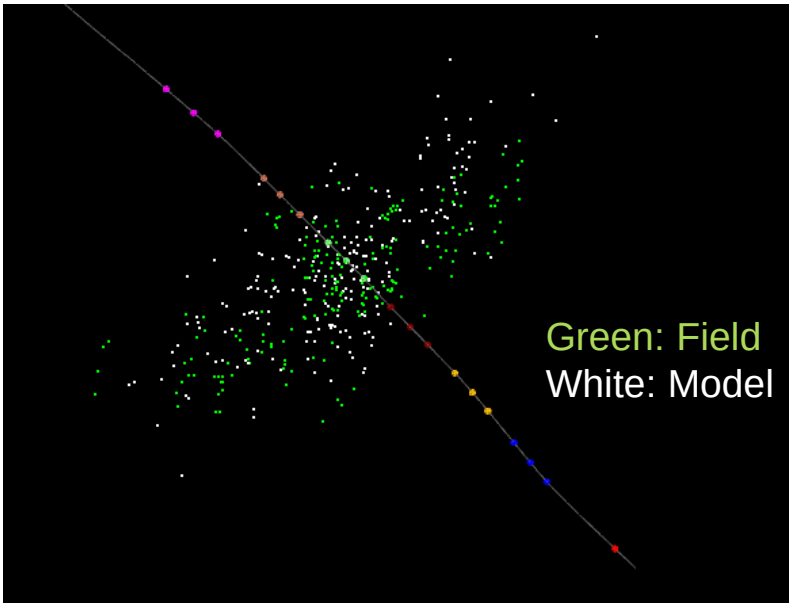

Figure 3. Map view of the simulated (white) and observed (green) microseismicity.

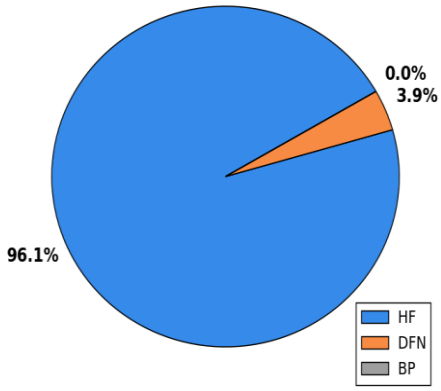

Figure 4. Percentage of the fracturing fluid in different portions of the fracture network.

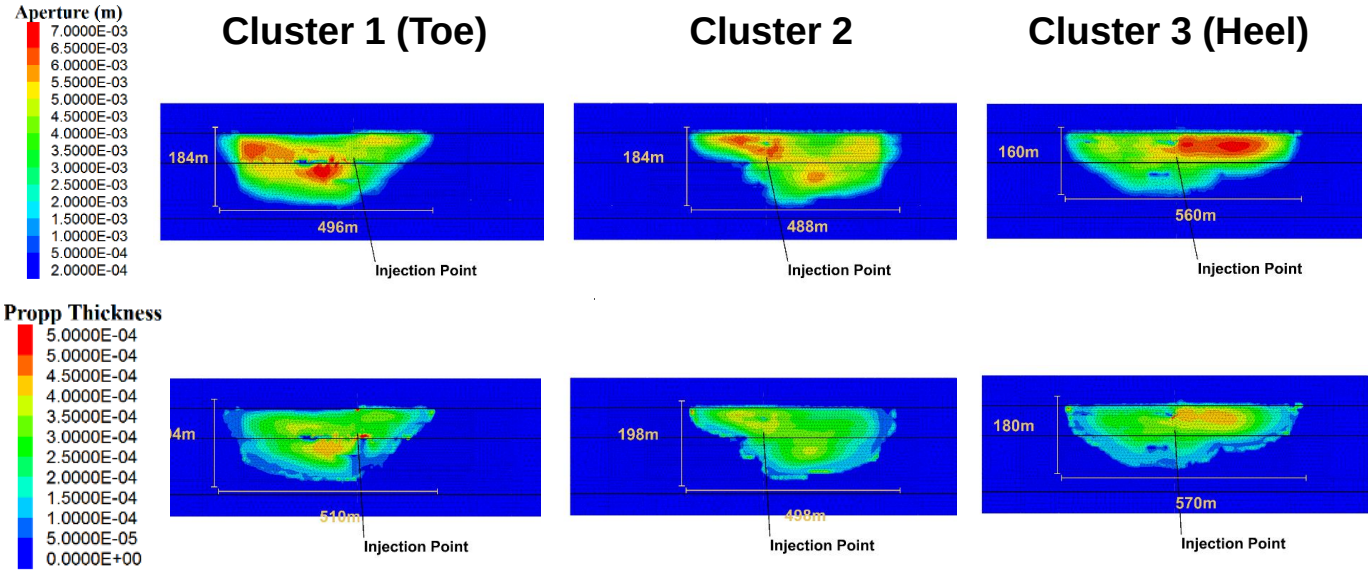

Figure 5. Primary fracture planes for the three clusters showing aperture (top row) and proppant thickness/concentration (bottom row).

Conclusions

The production and reservoir drainage can be estimated from a calibrated fracture model by performing a reservoir simulation, using enhanced permeability proportional to the proppant concentration. Alternatively, the product of the fracture surface contact area and some reservoir quality metric (e.g. hydrocarbon pore volume) can be used to compare different completion options. Proppant concentration thresholds can also be used to identify the propped portion of the fracture to limit the fracture contact area to where the permeability would be enhanced. Different fracture designs (e.g. rate, fluid type and proppant schedule) can be compared to optimize the reservoir contact in the zone of influence and guide field tests. The well completion (e.g. number of perforation clusters and spacing) can be tested to investigate the potential impact of stress shadowing between competing adjacent fractures, along with potential well orientations to examine the impact of offset fracture initiation points relative to the stress field. Landing depth of the horizontal wells can be investigated to maximimize contact with the zone of interest. Similarly, stage spacing can be optimized. Ultimately well spacing can investigated, including the effective drainage offset from each lateral and potential hydraulic and mechanical interference during fracturing. The model described here is 3D and so the optimal well sequencing between laterals in different zones can also be explored.

Acknowledgements

The authors would like to acknowledge ConocoPhillips for their permission to show results of this study.

References

Damjanac, B., and P. Cundall, 2014, Application of Distinct Element Methods to Simulation of Hydraulic Fracturing in Naturally Fractured Reservoirs, in Recent Advances in Numerical Simulation of Hydraulic Fracture 2014.

Kohli, A.H., and M. D. Zoback, 2013, Frictional Properties of Shale Reservoir Tocks, *J. Geophys. Res. Solid Earth, 118*, doi:10.1002/jgrb.50346

Maxwell, S.C., M. Mack, F. Zhang, D. Chorney, S.D. Goodfellow and M. Grob, 2015, Differentiating Wet and Dry Microseismic Events Induced During Hydraulic Fracturing, URTeC, 2154344.

Rodinov, Y., R. Parker, M. Jones, Z. Chen, S. Maxwell, and L. Matthews, 2012, Optimization of Stimulation Strategies using Real-Time Microseismic Monitoring in Horn River Basin: GeoConvention 2012, CSEG, Expanded Abstracts.